Substrate influence on the shape of domains in epitaxial PbTiO(3) thin films

Venkatesan, Sriram; Kooi, B. J.; De Hosson, J. T. M.; Vlooswijk, A. H. G.; Noheda, B.

Published in:
Journal of Applied Physics

DOI:
10.1063/1.2815657

Substrate influence on the shape of domains in epitaxial $PbTiO_3$ thin films

Sriram Venkatesan, B. J. Kooi,[a] and J. T. M. De Hosson
Department of Applied Physics, Zernike Institute for Advanced Materials and the Netherlands Institute for Metals Research, University of Groningen, Nijenborgh 4, 9747 AG, Groningen, The Netherlands

A. H. G. Vlooswijk and B. Noheda
Department of Chemical Physics, Zernike Institute for Advanced Materials, University of Groningen, Nijenborgh 4, 9747 AG, Groningen, The Netherlands

(Received 5 July 2007; accepted 23 September 2007; published online 19 November 2007)

Epitaxial $PbTiO_3$ thin films were grown on $SrTiO_3(001)$ and $DyScO_3(110)$ substrates by pulsed laser deposition. We used high-resolution transmission electron microscopy to investigate the 90° domain structure in the films. They were found to have a predominant fraction of *c* domains along with a certain minor volume fraction of *a* domains that is clearly higher in case of the $DyScO_3$ substrates. In $PbTiO_3$ on $SrTiO_3$ the *a* domains were found to have a wedge shape, whereas in $PbTiO_3$ on $SrRuO_3/DyScO_3$ they have a nearly uniform width. The presence of steps in the domain walls has been observed in the films on both substrates, but the steps are clearly more dominant in the case of $SrTiO_3$ than of $SrRuO_3/DyScO_3$ and are responsible for the observed wedge shape. The observed difference in the films induced by the two substrates is attributed to a higher stiffness of $SrTiO_3$ than of $SrRuO_3/DyScO_3$ as we corroborated with nanoindentation experiments. © *2007 American Institute of Physics*. [DOI: 10.1063/1.2815657]

I. INTRODUCTION

Ferroelectric thin films have attracted major attention in recent years because of their applications in integrated ferroelectric devices such as nonvolatile memories,[1] ultrasonic sensors,[2] and infrared detectors.[3] In the last decade, research of ferroelectric thin films has particularly been focused on $PbTiO_3$, $BaTiO_3$, $Pb(Zr_{1-x}Ti_x)O_3$, and $BaSr_{1-x}Ti_xO_3$.[4,5] Thin films of these oxide materials have been deposited by molecular beam epitaxy, sputtering, pulsed laser deposition (PLD), and low cost chemical solutions methods like sol-gel dip coating, spin coating.[6] Each one of these techniques has its own limitations. PLD has several advantages relative to the other methods, i.e., complex oxides can be grown with proper stoichiometry, the growth rate can be controlled accurately, and it is possible to use a multitarget system. We employed PLD for growth of $PbTiO_3$ thin films on two different substrates, namely $SrTiO_3$ and $DyScO_3$. $PbTiO_3$ can be grown coherently on $SrTiO_3$ because of its good lattice match compared to most other substrates. Substrates belonging to the scandates family became a recent choice because of their perovskite structure with lattice parameters around 3.95 Å, which offers a new range of misfit-strain values for some well-known ferroelectric perovskites such as $PbTiO_3$.[7,8]

At room temperature, the mismatch between the *a* axis of tetragonal $PbTiO_3$ (PTO) and the lattice constant of $SrTiO_3$ (STO) is $\sim 0.2\% - 0.3\%$ with $a_{PTO} \approx a_{STO} \ll c_{PTO}$ and in case of $DyScO_3$ (DSO) the mismatch is about 1.4% with $a_{PTO} < a_{DSO} \ll c_{PTO}$. This situation is reversed at the growth temperature (e.g., 570 °C), where the mismatch between cubic PTO and DSO is negligibly small, whereas that of cubic PTO on STO increases to about 1% (with $a_{STO} < a_{PTO}$). This mismatch together with the difference in thermal expansion of the substrate and the film generally gives rise to a polydomain structure (where the dominant fraction consists of *c* domains and the minor fraction of *a* domains) and/or strain relieving dislocations, i.e., misfit and threading dislocations.[9–11] However, from the application point of view it is generally desired to have the tetragonal film with its *c* axis oriented exclusively normal to the substrate surface, so that the spontaneous polarization is normal to the surface. Although ferroelectric thin films were prepared and applied with remarkable progress in the last decade, the basic problem of 90°-domain formation generally persisted, at least for the thicker films, and still requires in-depth analyses. The presence of 90° domains in $PbTiO_3$ films deposited by the PLD technique on different substrates like $SrTiO_3$, MgO, $KTaO_3$, and $LaAlO_3$ has been reported, particularly in the mid-1990s, in several studies, e.g., focusing on the volume fraction of *a* domains as a function of substrate type and film thickness.[12–14]

Our $PbTiO_3$ films are grown at 570 °C, in order to allow sufficient thermal activation (e.g., atomic mobility, diffusion, etc.) and avoid unwanted pyrochlore phase formation. This deposition temperature is above the ferro- to paraelectric transition temperature T_C of bulk $PbTiO_3$ (490 °C). However, recent experimental studies have shown (in accordance with earlier theoretical work[15]) that, if the films are strained during deposition, T_C can be pushed to substantially higher temperatures than that of the bulk.[16–18] Accordingly, our $PbTiO_3$ films on $SrTiO_3$ (at 570 °C) should grow directly in the tetragonal ferroelectric phase. In contrast, cubic $PbTiO_3$ films on $DyScO_3$ grow without significant mismatch at the deposition temperature and therefore grow in the paraelectric phase. Upon cooling from the cubic paraelectric phase to the

[a]Author to whom correspondence should be addressed. Electronic mail: b.j.kooi@rug.nl

tetragonal ferroelectric phase 90° domains develop in the $PbTiO_3$ on $DyScO_3$. In the case of $PbTiO_3$ on $SrTiO_3$ no *a* domains should, in principle, be expected since for all temperatures the *a* axis of tetragonal $PbTiO_3$ remains well matched with the lattice constant of $SrTiO_3$. This is indeed the case when the films are grown under conditions close to thermodynamic equilibrium, as will be elaborated in another paper.[19] A similar result was recently found for $PbZr_{0.2}Ti_{0.8}O_3$ on $SrTiO_3$.[20] In the present work, we deliberately introduced *a* domains in $PbTiO_3$ on $SrTiO_3$ by changing the deposition parameters.

In this paper, we particularly focus our attention on the shape of *a* domains in $PbTiO_3$ thin films, which has not been studied in detail in the past, as influenced by the substrate stiffness. High-resolution transmission electron microscopy (TEM) has been employed to image the *a* domains and nanoindentation experiments were performed in order to allow a correlation with the substrate stiffness.

II. EXPERIMENTAL

Pulsed laser deposition was used to grow a 110 nm film of $PbTiO_3$ on (001) $SrTiO_3$ and two 30 nm films on (110) $DyScO_3$ with 5 and 30 nm $SrRuO_3$ conductive perovskite as the intermediate layer. The bulk lattice parameters of $PbTiO_3$ are [at room temperature (RT)] $a=b=3.894$ Å and $c=4.140$ Å,[21] i.e., with a tetragonal structure. $SrTiO_3$ has a cubic structure and its lattice constant is (at RT) $a=3.905$ Å. The $DyScO_3$ has an orthorhombic structure with the following lattice constants (at RT): $a=5.440$ Å, $b=5.713$ Å, and $c=7.887$ Å.[22] (110)-oriented $DyScO_3$ has nearly a square in-plane lattice with $a_{\parallel}=3.944$ Å.

The $SrTiO_3$ substrates were ultrasonicated with ultrapure water, then the surfaces were etched using buffered HF, and finally heat treated at 960 °C for 1.5 h. The substrates we used were predominantly, but not completely, terminated by titanium oxide as was inferred from atomic force microscopy analysis. The $DyScO_3$ substrates were cleaned with ethanol, acetone, and thermally treated at a temperature of 960 °C for about an hour. The substrates were glued to the heater using silver paste. $PbTiO_3$ films were deposited on $SrTiO_3$ at a temperature of 570 °C using a pulsed KrF excimer laser at a wavelength of 248 nm (Lambda Physik COMPex pro 205) in an ambient oxygen pressure of 0.13 mbar with a repetition rate of 10 Hz. A temperature above 600 °C will lead to evaporation of lead. Our target is of the right stoichiometry without any excess percentage of lead. The substrates were kept at a distance of 51 mm from the target. An energy density of 2.5 J/cm^2 with a laser spot of ~3 mm^2 was used. After deposition, the films were annealed within oxygen of 0.5 bar and cooled at the rate of 5 °C/min. The films on $DyScO_3$ were deposited with a slightly less energy density of 2 J/cm^2 and a substrate target distance of 45 mm with a repetition rate of 1 Hz; the other parameters were identical as for $PbTiO_3$ growth on $SrTiO_3$. The intermediate $SrRuO_3$ layer was grown at a temperature of 600 °C with 2 Hz repetition rate.

X-ray diffraction was used to determine the presence, amount, and orientation (tilting) of *c* and *a* domains in the thin films of $PbTiO_3$ on both substrates. Because of the orientation of both types of domains (and the overlap with substrate peaks), simple $\theta-2\theta$ scans are insufficient to determine their presence. By performing measurements on both the $\theta-2\theta(K_{\parallel})$ and $\omega(K_{\perp})$ axes, reciprocal space maps[23,24] were obtained using a standard laboratory diffractometer (X'Pert Panalytical, Cu anode $\lambda=1.540598$ Å), providing detailed information about the *a* and *c* domains.

High-resolution TEM was used to investigate the cross-sectional structure of the films. TEM samples were prepared by the conventional method involving cutting, grinding, polishing, dimpling, and ion milling. A precision ion polishing system (Gatan model 691) with 4 kV Ar^+ beams having an incident angle of 8° on both sides was used. The observations were performed with a JEOL 2010F electron microscope operating at an accelerating voltage of 200 kV.

Nanoindentations experiments were performed with a calibrated MTS Nano Indenter® XP with a continuous stiffness module (CSM). A Berkovich-type indenter was used and the data were obtained during loading using the CSM. The indentations were all performed up to a maximum depth of 1500 nm; the superimposed force frequency for the CSM was 45 Hz. The final results were obtained by averaging over ten indentations and a depth range of 400–1400 nm. To allow an accurate direct comparison, an identical procedure for indentations was performed on both the (001) $SrTiO_3$ and (110) $DyScO_3$ substrates. To obtain the Young's moduli from the reduced moduli, a Poisson ratio (ν) of 0.24 was used. This value holds for $SrTiO_3$ as based on the single crystal elastic constants.[25]

III. RESULTS

Examples of the x-ray diffraction (XRD) results of $PbTiO_3$ films on both substrates, $SrTiO_3$ and $DyScO_3$, are presented in Fig. 1. $\theta-2\theta$ scans of $PbTiO_3$ on both types of substrates are shown in Fig. 1(a) and reveal that unwanted (impurity) phases are not detectable in the grown films. By performing scans around different Bragg peaks the presence of *a* domains in the $PbTiO_3$ films next to dominant *c* domains on both substrates was confirmed. The reciprocal space map around the 001 Bragg peak of the (30 nm) $PbTiO_3$ film on $DyScO_3$ (with 30 nm intermediate $SrRuO_3$), shown in Fig. 1(b), clearly indicates that the *a* and *c* domains exhibit a long range ordered structure, i.e., an alternating *c*-*a* structure with a periodicity of 28 nm.[26] For the $PbTiO_3$ film on $SrTiO_3$ the XRD measurements did not reveal any ordering of the domain structure.

A cross-sectional bright-field TEM image of a 110 nm $PbTiO_3$ film on $SrTiO_3$ is shown in Fig. 2. The presence of wedge-shaped *a* domains, with decreasing widths when approaching the substrate, can be observed clearly in the image. Special care was taken that a sample tilt was not responsible for the observed shape of the domains. Although the *a* domains seem to exhibit a periodicity in the image, a proper short or long range order is not present, in agreement with the XRD observations. The apex of the wedge-shaped *a* do-

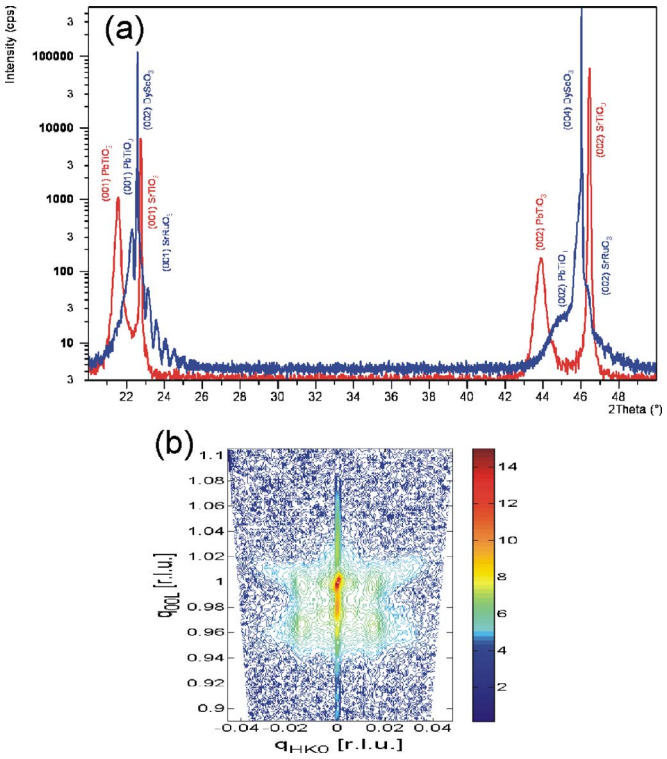

FIG. 1. (Color online) X-ray diffraction patterns showing in (a) $\theta-2\theta$ scans of $PbTiO_3$ on $SrTiO_3$ (red) and of $PbTiO_3$ on $DyScO_3$ (blue) and in (b) a reciprocal space map around the (001) reflection of $PbTiO_3$ on $DyScO_3$ in units of $2K_0=4\pi/\lambda=4\pi/1.540598$ Å.

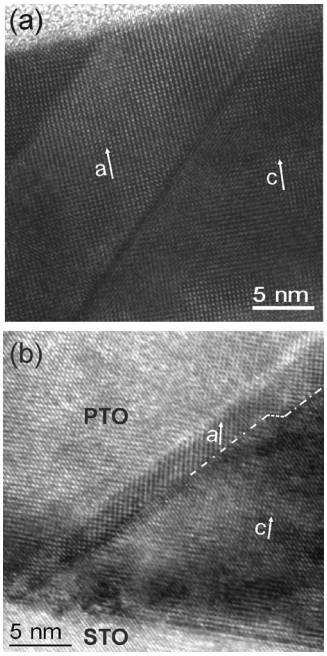

FIG. 3. High-resolution TEM images showing details of the *a* domains in the 110 nm $PbTiO_3$ film on $SrTiO_3$ with in (a) the region near the top of the film and in (b) the region near the bottom of the film, indicating the wedge shape of the *a* domains. The domain walls are formed by parallel (101) planes of the *a* and *c* domains which match strain free. The wedge shape is introduced by (100) and (001) steps in the domain walls, which are not strain free. A relative large step can be identified and is indicated in Fig. 3(b).

mains is not always located at the substrate-film interface. It has been observed that domains start from dislocations within the film that stand off the interface.

High-resolution TEM images of the same sample are shown in Fig. 3. Despite the overall wedge shape it can be clearly seen in the image that the domain walls are predominantly formed by parallel (101) planes of the *a* and *c* domains. Walls are in this way strain free. However, in order to form the wedge shape, steps formed by (100) and (001) are present in the domain wall. A clear example of a relative large step is given in Fig. 3(b) [and another clear example of steps is given later in Fig. 6(b)]. These steps are not strain-free and the reasons for them to arise will be presented in the discussion.

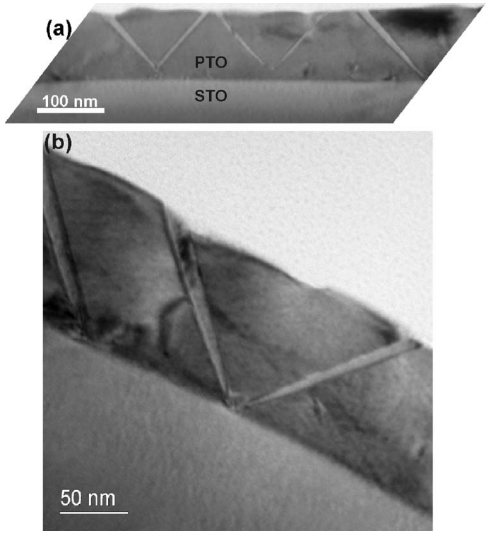

FIG. 2. Bright-field TEM images of a 110 nm $PbTiO_3$ film on $SrTiO_3$ showing the presence of wedge-shaped *a* domains. (a) Overview image in which also some dislocation contrast within the film is visible. (b) More detailed view of wedge-shaped *a* domains.

On the basis of Fourier transforms taken from the high-resolution images around *a* domains, see the example in Fig. 4, more details about the crystal structures in the two types of domains and their mutual orientation can be obtained. It is found that, within experimental accuracy, the *a* and *c* axis of both *a* and *c* domains are still orthogonal. The predicted tilt of the unit cell within the *a* domain with respect to the one in the *c* matrix of the lead titanate film, calculated from $90°-2\tan^{-1}(a/c)\approx 3.5°$, is not achieved in the case of $SrTiO_3$ substrates, but $4.7°\pm 0.5°$ is found experimentally. The experimental c/a ratio is 1.07 ± 0.01 for the *c* domain and 1.09 ± 0.01 for the *a* domain, which in the latter case is significantly larger than the theoretical value of 1.063. However, the experimentally found larger tilt is consistent with the larger c/a ratio. A similar observation of a too large tilt between the *a* and *c* domains has been reported previously and was explained in terms of a vicinal (tilted) surface before growth that produces unequal populations in the possible orientations of the *a* domains.[27] This explanation would imply that we measured in "uphill" *a* domains that became predominantly populated. The miscut of the $SrTiO_3$ substrate we used was $0.1°-0.3°$, indicating that unit cell high steps occur about each 100 nm lateral scale. The observed *a*-domain

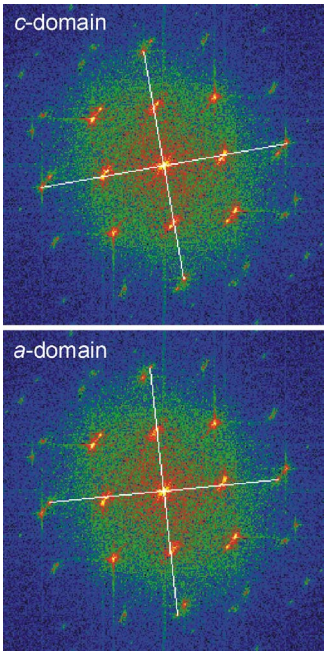

FIG. 4. (Color online) Fourier Transform taken from a selected part (256 $\times$256 pixels) around an *a* domain in a HRTEM image. The top image shows the *a*-domain orientation and the bottom image the *c* domain. From such transforms it can be inferred that (within the accuracy limits) the *a* and *c* axes are still orthogonal in the *a* and *c* domains, that the *c*/*a* ratio is 1.07±0.01 and 1.09±0.01 for the *c* and *a* domains, respectively, and that their mutual tilt is 4.7° ±0.5°.

density is in rough agreement with this step density. The miscut of the $DyScO_3$ substrates we used was smaller, i.e., 0.05°–0.1°.

A cross-sectional bright-field TEM image of a 30 nm $PbTiO_3$ film on $DyScO_3$ substrates with a 5 nm $SrRuO_3$ intermediate layer is shown in Fig. 5. Regions with parallel oriented and nearly regularly spaced *a* domains can be observed. The volume fraction of the *a* domains is found to be clearly higher for the $PbTiO_3$ films on $DyScO_3$ than for these films on $SrTiO_3$; about 20–25 vol % versus less than 10%. Based on the lattice constants at room temperature a clearly smaller mismatch holds for a *c*-oriented $PbTiO_3$ film on $SrTiO_3$ than on $DyScO_3$, about −0.26% and −1.4%, respectively. Even when the strains are relaxed at the growth temperature, after cooling the mismatch remains smaller for $SrTiO_3$ than for $DyScO_3$. These misfits correspond to a tensile strain within the film that can be relieved by the formation of *a* domains. Due to the larger mismatch in case of the $DyScO_3$ substrate a higher volume fraction of *a* domains can be expected. Note, however, as explained in the Sec. I that, if $PbTiO_3$ film on $SrTiO_3$ are grown under conditions closer to thermodynamic equilibrium, *a* domains are not observed at all.[19]

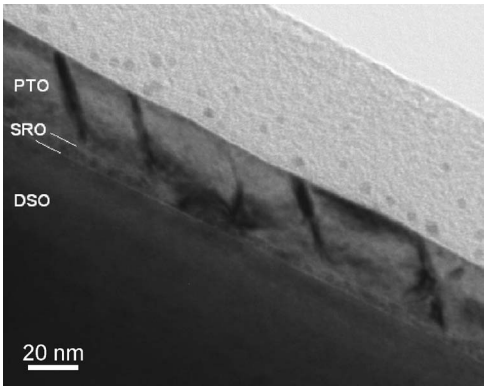

FIG. 5. Bright-field TEM image of a 30 nm $PbTiO_3$ film on $DyScO_3$ (with a 5 nm intermediate $SrRuO_3$ layer) showing the presence of a nearly regularly spaced array of *a* domains within the $PbTiO_3$ film.

A careful analysis of $PbTiO_3$ on atomically flat $DyScO_3$ substrates indicates that the *a* domains have a clear tendency of having a width of about 6 nm,[26] but in rare cases in the earlier sample even domains with a width of only 2 nm have been observed. The distance between neighboring *a* domains is typically 28 nm, however, some clear variations in distances (typically ±10 nm) are also observed within the sample. In the similar sample where a 30 nm $SrRuO_3$ intermediate layer was used the preferred width of 6 nm of the *a* domains and a periodic spacing of about 28 nm between them was observed to hold more strongly.[26] Also in the XRD measurements clear proof of a very similar ordered distance between the *a* domains could be found on the basis of satellite peaks [cf. Fig. 1(b)]. These differences are probably related to a different substrate quality, i.e., variations in substrate treatment, since the presence of steps in the substrate disturbs the domain periodicity.

High-resolution TEM images of the sample with the 30 and 5 nm intermediate $SrRuO_3$ layers are shown in Figs. 6(a) and 6(b), respectively. In general, the two domain walls of the *a* domain tend to be quite parallel for $PbTiO_3$ on $DyScO_3$ [cf. Figs. 6(a)]; the domains have clearly less wedge shape than in the case of the $SrTiO_3$ substrate. However, the example given in Fig. 5(b), where the intermediate $SrRuO_3$ layer is 5 nm, shows clear steps in the domain wall. Although the statistics are poor, we observed that in the case of only 5 nm intermediate $SrRuO_3$ layer steps in the domain wall are present, whereas such steps were not detected in case of the 30 nm $SrRuO_3$ layer. The *c*/*a* ratio within the $PbTiO_3$ derived from high-resolution TEM (HRTEM) images of the *c* domains is 1.07 (±0.01) which is in agreement with the theoretical value of 1.063. We obtained 3.8° for the tilt between the unit cells in the *a* and *c* domains which is also close to the theoretical value of 3.5°.

Interestingly, we found clear differences in functional properties, as measured with piezoresponse force microscopy, for these different types of $PbTiO_3$ films on $DyScO_3$ that we attributed to this different step density in the domain walls.[28]

IV. DISCUSSION

The most striking effect observed in the present work is the observed difference in the shape of the *a* domains in the $PbTiO_3$ films depending on the substrate type; on $SrTiO_3$ the domains clearly always have a wedge shape, whereas on $SrRuO_3/DyScO_3$ they show a clearly more uniform width. An exaggerated schematic representation of the two cases is shown in Fig. 7. The corresponding difference in step density

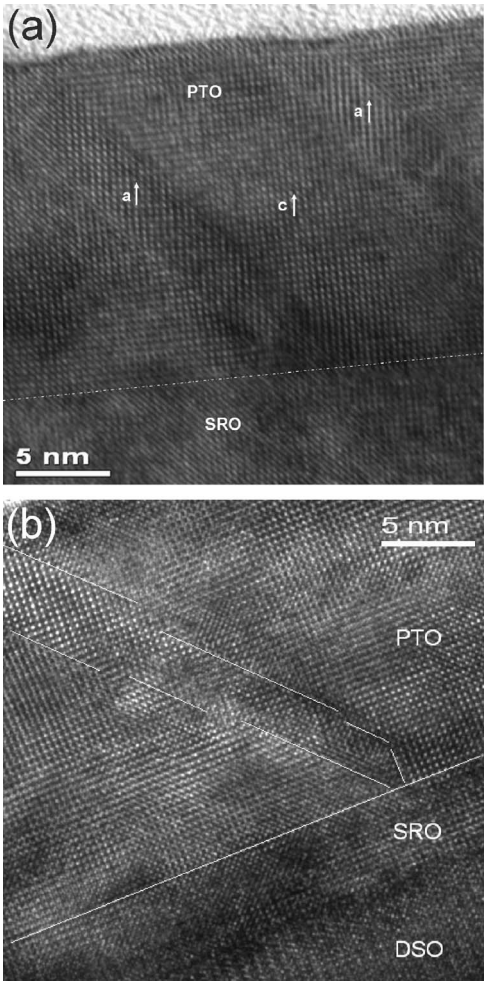

FIG. 6. High-resolution TEM images showing details of the *a* domains in the 30 nm $PbTiO_3$ films on $DyScO_3$. (a) Two closely spaced *a* domains with a uniform width of about 5 nm in the $PbTiO_3$ film with a 30 nm intermediate $SrRuO_3$ layer. (b) Example of a wedge-shaped *a* domain in the $PbTiO_3$ film with a 5 nm intermediate $SrRuO_3$ layer.

in the domain wall can be explained by the difference in stiffness of the substrates (in conjunction with sufficient adhesion across the substrate film interface).

For the *c* domains the (001) plane is parallel to the interface, but for the *a* domains in principle the tilt of 3.5° holds between the substrate surface and the (100) [or (010)] plane. The "defect" accounting for this local misorientation can in analogy be called a misfit disclination.[9] The strains associated with this disclination create the tendency to minimize the width of the *a* domains. However, for strain accommodation within the film *a* domains are required. Overall, a

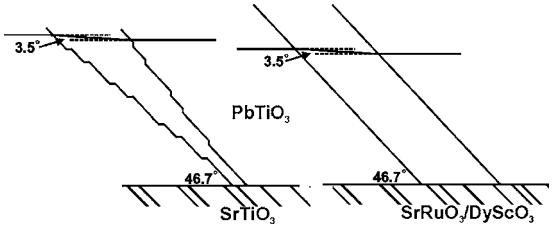

FIG. 7. Schematic representation of the wedge-shaped *a* domains in $PbTiO_3$ films on $SrTiO_3$ on the left and *a* domains with a uniform width in $PbTiO_3$ films on $DyScO_3$ on the right.

strain-energy balance will hold. In fact, this balance will prevent the formation of *a* domains below a critical thickness in accordance with theory[29] and experiments.[26] Above the critical thickness these domains can develop, but nevertheless the interface strains will tend to keep the domains in most cases thinner near the interface than in the bulk. To minimize domain-wall energy, in principle, thick *a* domains would be expected, but these are not found due to the interfacial clamping strain. Clearly away from the interface the *a* domains have the tendency to have a width corresponding to $c/\sin\alpha$,[26] where α is the tilt mentioned several times earlier [which is $90°-2\tan^{-1}(a/c)$]. In this way the planes parallel to the interface in the *c* domains on both sides of the *a* domain match coherently with the slightly tilted plane in the *a* domain. If the clamping strain energy at the interface of an *a* domain is higher than the strain energy associated with steps in the domain wall, then a wedge-shaped *a* domain with smaller width near the interface will result. Apparently this situation holds in case of the $SrTiO_3$ substrate. In the case of $DyScO_3$ with $SrRuO_3$ as an intermediate layer the interface clamping strain energy is apparently less and the steps in the domain wall tend to run all the way to the interface and form domains with nearly uniform width. This difference in clamping strain energy is due to a difference in stiffness of the substrate, where a higher stiffness causes more strain energy.

Therefore, knowledge of the elastic constants of $SrTiO_3$ and $DyScO_3/SrRuO_3$ can give support to the earlier scenario. From the dependence of the electric constants on electric field,[30] it appears that $SrTiO_3$ is not completely ionic but that the TiO_3 building blocks are partially covalently bound. On the other hand, the scandium group having the outer electronic configuration d^1s^2 loses its *d*-electron character in the III oxidation state and the scandium group can be regarded as forming a transitional region between the *s* elements and the main *d* block. Likewise, the behavior of the lanthanide elements such as $Dy(4f^{10}5d^06s^2)$ is that of a III state and the behavior is very similar to that of the scandium group. It is therefore expected that the ionicity of $DyScO_3$ is higher than of $SrTiO_3$. Because covalent bonds are stiffer than ionic bonds, we expect that $DyScO_3$ is more compliant than $SrTiO_3$. Similarly, one might expect that the metallic (conducting) character of $SrRuO_3$ implies a relative soft material.

Interestingly, these qualitative arguments give the right sequence when quantitative stiffness data are considered. Most data are available for $SrTiO_3$. Based on single crystal elastic constants a Young's modulus *E* (along the cube axis) ranging from 265 to 303 GPa and a shear modulus *G* ranging from 119 to 127 GPa has been reported in four independent experiments.[25,30,31] Nanoindentation experiments gave a somewhat lower value for E: 225 ± 14 GPa.[32] For $SrRuO_3$ only a single reference was found pertaining to a polycrystalline sample giving $E=161$ GPa and $G=60.1$ GPa.[33] These values are much lower than the ones that hold for $SrTiO_3$, cannot be attributed to anisotropy (i.e., polycrystal versus single crystal) and indicates that $SrTiO_3$ is indeed much stiffer than $SrRuO_3$. For $DyScO_3$ unfortunately it seems that data on elastic constants have not been published. Therefore, we performed nanoindentations with a calibrated

MTS Nano Indenter® XP with a CSM. For $DyScO_3$ we obtained $E=250\pm3$ GPa and for $SrTiO_3$ we found 279 ± 4 GPa.[34] These results indeed show that $SrTiO_3$ is the stiffest material, $DyScO_3$ about 10% less and $SrRuO_3$ is the most compliant one of the three.

Based on the relative stiffness of these three materials, the experimental findings regarding the step density in the domain walls can now be fully understood. The high stiffness of $SrTiO_3$ causes a high interfacial clamping strain energy leading to wedge-shaped *a* domains with small width near the interface. Since the typical width of an *a* domain is 6 nm the deformation field due to the interfacial clamping strain will extend, according to St. Venant's principle,[35] not more than a few times this value into the substrate. This means that when a 30 nm intermediate $SrRuO_3$ layer is used, the stiffness of the $DyScO_3$ is not relevant. On the other hand, when the intermediate $SrRuO_3$ layer has a thickness of only 5 nm also the stiffness of $DyScO_3$ comes into play. Based on these considerations, it can now be understood that the *a* domains in the $PbTiO_3$ on the 30 nm $SrRuO_3$ showed most uniform width because it makes use of the most compliant $SrRuO_3$ in reducing the stress fields in $PbTiO_3$ and that, in case of the 5 nm $SrRuO_3$ film, a higher step density in the domain walls is found (because it experience the stiffer $DyScO_3$), but the domains are most clearly wedge shaped in the case of $SrTiO_3$ being the stiffest material of the three.

Note that in all these cases it is assumed that the adherence between film and substrate is sufficient, because when the adherence is poor, the interfacial clamping strain will always be low, independent of the stiffness of the substrate, and *a* domains with uniform width will result. In this respect it is also worth it to mention that a strong adherence between $PbTiO_3$ and $SrTiO_3$ is facilitated by the continuation of the titanate sublattice across the interface. Finally, it is important to note that the present study on the shape of *a* domains is not merely of structural interest because we have also strong indications that the relative step density in the domain walls of the $PbTiO_3$ has a direct impact on the functional properties of this ferroelectric material.[28]

V. CONCLUSIONS

Domain structures of the $c/a/c$ type have been observed in $PbTiO_3$ films on $SrTiO_3$ and $DyScO_3$ substrates, where the *a* domains are present with a clearly higher volume fraction (20–25 vol % versus less than 10 vol %) and are more regularly spaced in the $PbTiO_3$ films on $DyScO_3$. The higher volume fraction can be directly related to the larger mismatch at the interface between $PbTiO_3$ and $DyScO_3$ than between $PbTiO_3$ and $SrTiO_3$.

A striking finding is that the shape of the *a* domains depends sensitively on the substrate type. On $SrTiO_3$ wedge-shaped *a* domains are found, whereas on $DyScO_3$ *a* domains with generally uniform width are observed. The wedge shape of the *a* domains is found to be introduced by (100) and (001) steps in the domain walls which further predominantly consist of parallel (101) planes of the adjacent *a* and *c* domains. These (101) planes match strain-free, whereas the steps in the wall cause local strains.

The reason for the developments of wedge-shaped *a* domains can be understood taking the clamping strain at the interface into account. When the interfacial clamping strain energy is higher than the strain energy associated with steps in the domain wall, wedge-shaped *a* domains will be formed. The different shapes of the *a* domains on the different substrate types can be explained by the higher stiffness of $SrTiO_3$ compared to $SrRuO_3/DyScO_3$ causing for the former system a higher interfacial clamping strain energy and thus a higher probability that steps are formed in the domain wall reducing the domain width near the interface.

ACKNOWLEDGMENTS

Financial support from the Zernike Institute for Advanced Materials and the Netherlands organizations for research FOM and NWO is gratefully acknowledged. Arjen Janssens and Beatriz Barcones, both of the Inorganic Materials Science group, University of Twente, The Netherlands, are gratefully acknowledged for providing the $PbTiO_3/DyScO_3$ samples and for preparation of a cross-sectional TEM sample, respectively.

[1] O. Auciello, J. F. Scott, and R. Ramesh, Phys. Today **51**, 22 (1998).
[2] G. H. Haertling, Am. Ceram. Soc. Bull. **73**, 93 (1994).
[3] R. W. Whatmore, P. C. Osband, and N. M. Shorrocks, Ferroelectrics **68**, 351 (1987).
[4] S. Yoon, J. Lee, and A. Safari, J. Appl. Phys. **76**, 2999 (1994).
[5] R. Waser, Integr. Ferroelectr. **15**, 39 (1997).
[6] K. D. Budd, S. K. Dey, and D. A. Payne, Br. Ceram. Proc. **36**, 107 (1985).
[7] M. D. Biegalski, J. H. Haeni, S. Trolier-McKinstry, D. G. Schlom, C. D. Brandle and A. J. Ven Graitis, J. Mater. Res. **20**, 952 (2005).
[8] G. Catalan, A. Janssens, G. Rispens, S. Csiszar, O. Seeck, G. Rijnders, D. H. A. Blank, and B. Noheda, Phys. Rev. Lett. **96**, 127602 (2006).
[9] J. S. Speck, A. C. Daykin, A. Seifert, A. E. Romanov, and W. Pompe, J. Appl. Phys. **78**, 1696 (1995).
[10] J. S. Speck and W. Pompe, J. Appl. Phys. **76**, 466 (1994).
[11] J. S. Speck, A. Seifert, W. Pompe, and R. Ramesh, J. Appl. Phys. **76**, 477 (1994).
[12] B. S. Kwak, A. Erbil, J. D. Budai, M. F. Chisholm, L. A. Boatner, and B. J. Wilkens, Phys. Rev. B **49**, 14865 (1994).
[13] S. Stemmer, S. K. Streiffer, F. Ernst, M. Ruhle, W.-Y. Hsu, and R. Raj, Solid State Ionics **75**, 43 (1995).
[14] W. Y. Hsu and R. Raj, Appl. Phys. Lett. **67**, 792 (1995).
[15] N. A. Pertsev, A. G. Zembilgotov, and A. K. Tagantsev, Phys. Rev. Lett. **80**, 1988 (1998).
[16] P. E. Janolin, F. Le Marrec, J. Chevreul, and B. Dkhil, Appl. Phys. Lett. **90**, 192910 (2007).
[17] P. E. Janolin, B. Fraisse, F. Le Marrec, and B. Dkhil, Appl. Phys. Lett. **90**, 212904 (2007).
[18] S. Gariglio, N. Stucki, J.-M. Triscone, and G. Triscone, Appl. Phys. Lett. **90**, 202905 (2007).
[19] S. Venkatesan, B. J. Kooi, A. Morelli, G. Palasantzas, J. T. M. De Hosson, A. H. G. Vlooswijk, and B. Noheda (unpublished).
[20] I. Vrejoiu, G. Le Rhun, L. Pintilie, D. Hesse, M. Alexe, and U. Gösele, Adv. Mater. **18**, 1657 (2006).
[21] G. Shirane, S. Hushino, and K. Suzuki, Phys. Rev. **80**, 1105 (1950).
[22] J. H. Haeni *et al.*, Nature (London) **430**, 758 (2004).
[23] P. van der Sluis, J. Phys. D **26**, A188 (1993).
[24] Q. Gan, K. Wasa, and C. B. Eom, Mater. Sci. Eng., B **56**, 204 (1998).
[25] Y. L. Li, S. Choudhury, J. H. Haeni, M. D. Biegalski, A. Vasudevarao, A. Sharan, H. Z. Ma, J. Levy, V. Gopalan, S. Trolier-McKinstry, D. G. Schlom, Q. X. Jia, and L. Q. Chen, Phys. Rev. B **73**, 184112 (2006).
[26] A. H. G. Vlooswijk, B. Noheda, G. Catalan, A. Janssens, B. Barcones, G. Rijnders, D. H. A. Blank, S. Venkatesan, B. Kooi, and J. T. M. De Hosson, Appl. Phys. Lett. **91**, 112901 (2007).

[27]C. D. Theis and D. G. Schlom, Proceedings of the Tenth IEEE International Symposium on Applications of Ferroelectrics, 1996, Vol. 1, p. 491 (unpublished).
[28]A. Morelli, S. Venkatesan, G. Palasantzas, B. J. Kooi, and J. Th. M. De Hosson, J. Appl. Phys. **102**, pp. 084103 (2007).
[29]W. Pompe, X. Gong, Z. Suo, and J. S. Speck, J. Appl. Phys. **74**, 6012 (1993).
[30]R. O. Bell and G. Rupprecht, Phys. Rev. **129**, 90 (1963).
[31]E. Poindexter and A. A. Giardini, Phys. Rev. **110**, 1069 (1958).
[32]O. Bernard, M. Andrieux, S. Poissonnet, and A. M. Huntz, J. Eur. Ceram. Soc. **24**, 763 (2004).
[33]S. Yamanaka, T. Maekawa, H. Muta, T. Matsuda, S. Kobayashi, and K. Kurosaki, J. Solid State Chem. **177**, 3484 (2004).
[34]Simultaneously the hardness values for $DyScO_3$ and $SrTiO_3$ were obtained: 12.3 ± 0.3 GPa and 9.6 ± 0.3 GPa, respectively.
[35]J. N. Goodier, J. Appl. Phys. **13**, 167 (1942).